Interpretation of small-angle diffraction experiments on opal-like photonic crystals

F. Marlow,[1,2,*] M. Muldarisnur,[1] P. Sharifi,[1] and H. Zabel[3]

[1]*Max-Planck-Institut für Kohlenforschung, Kaiser-Wilhelm-Platz 1, DE-45470 Mülheim an der Ruhr, Germany*
[2]*Center for Nanointegration Duisburg-Essen (CeNIDE), University of Duisburg-Essen, Germany*
[3] *Department of Experimental Physics, Ruhr University Bochum, DE-44780 Bochum, Germany*

Comprehensive structural information on artificial opals involving the deviations from the strongly dominating face-centered cubic structure is still missing. Recent structure investigations with neutrons and synchrotron sources have shown a high degree of order but also a number of unexpected scattering features. Here, we point out that the exclusion of the allowed 002-type diffraction peaks by a small atomic form factor is not obvious and that surface scattering has to be included as a possible source for the diffraction peaks. Our neutron diffraction data indicate that surface scattering is the main reason for the smallest-angle peaks in the diffraction patterns.

Artificial opals are the most important approach to self-assembled photonic crystals (PhCs). They have frequently been characterized optically and by electron microscopy, revealing the strongly dominating dense-packed face-centered cubic (fcc) structure for some of the fabrication methods[1] such as vertical deposition (VD)[2,3] or the capillary deposition method (CDM)[4]. Other fabrication methods deliver large contents of random hexagonal packing,[5,6] hexagonal dense packing,[7] or even nondense packing;[8] but these opal-like systems seem to be less suited for application as photonic crystals. Regarding the fcc-dominated systems, one must, however, admit that the detailed structural understanding concerning defects, mosaic structure, domains, and their relations is still not complete. Classical methods for structure determination fail because of the small scattering angles. In addition, the mentioned structural properties depend on the details of the opal fabrication method, and therefore, a comparison of different investigations is often difficult.

In recent works, Sinitskii and Grigoriev *et al*. published a number of very interesting structure investigations using thermal neutrons and synchrotron radiation on VD-made samples.[9,10] These studies reveal a surprisingly high degree of order in the scattering pattern, but also deviations from the ideal picture. Also in former studies, the usefulness of diffraction studies was shown.[5,8]

In this Brief Report we will add two points to the current interpretation of the diffraction data. First, surface scattering has to be included as a possible source for diffraction peaks. Our neutron diffraction data for artificial opals fabricated by CDM indicate that surface scattering is the main reason for the lowest diffraction order. Second, the allowed 002-type diffraction peaks cannot be excluded from the discussion by a small atomic form factor.

Reviewing the published diffraction data and electron microscopy pictures of opals, one has two inconsistent impressions. On the one hand, a surprisingly high degree of order is shown. The lattice is well oriented[11] and the diffraction spots are sharp. Nearly perfect fcc lattices are visible in scanning electron microscopy (SEM); only very seldom can one recognize other lattices than fcc. On the other hand, there are peaks in the diffractograms which are not allowed, according to Bragg's law. In particular,

these are the peaks with smaller diffraction angles than the dominating $2\bar{2}0$-type peaks at normal incidence (see, e.g., Fig. 1).

Our experiments have been carried out at the SANS-2 beamline at the GKSS Geestacht. The neutron wavelength was 0.58 nm and the detector distance was 21.5 m. For the shown pictures, accumulation times of 1.3 and 10 h, respectively, were used delivering clear $2\bar{2}0$-diffraction spots with about 10^3 counts. Polystyrene (PS) opal films with a thickness of 25 μm were fabricated by the CDM (Refs. 4 and 12) and titania inverse opals by a procedure as described in Ref. 4 using these opal templates. CDM-made samples are very reproducible. Therefore, the pattern shown in Fig. 1(a) is representative for opals made by this method. The pattern in Fig. 1(b) depends slightly on fabrication details, which will be regarded in a separate publication.

A straightforward interpretation of the low-angle peaks in the diffraction patterns is the assignment to additional lattices mixed with the dominating, highly oriented fcc lattice.[9] However, neither the different lattices nor the transition regions between the different lattices have been convincingly found in SEM for VD-made or CDM-made samples. In addition, it is unclear why the dominating fcc lattice is so perfectly oriented,[11] while containing significant contaminations with other lattices. These contaminations can be expected to disturb the main lattice. Because of these inconsistencies it seems to be justified to also consider alternative explanations for the additional peaks instead of other lattices.

The number of unit cells in one crystal domain of a PhC is expected to be much smaller than in atomic crystals. Therefore, other effects, especially surface scattering, may gain importance. Finite-size effects which are strongly related to that have already been mentioned as a possible explanation for the inconsistencies.[10] Also, lattice imperfections typical for soft matter can generate quasiforbidden peaks,[13] however, very likely requiring a bit higher disorder than observed in CDM-made opals. Here, we estimate the magnitude of the surface effect, and for that we follow the standard procedure of introducing finite-size effects of the lattice.[14] A body function $B(r)$ for the semi-infinite space is chosen as in Ref. 15, but we treat it in a slightly different fashion. This treatment leads to a result similar to that in the standard crystal truncation rod
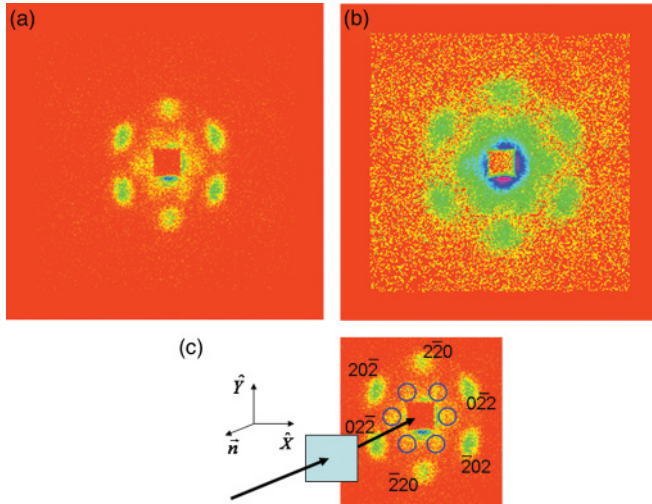
FIG. 1. (Color) (a) Neutron diffraction pattern for an opal film made by 264 nm PS spheres and (b) for a TiO_2 inverse opal film fabricated from a template, as in Fig. 1(a). The position of the peaks delivers lattice constants of 360 and 269 nm, respectively. (c) Scheme of the setup. The forbidden reflections are indicated by blue circles.

(CTR) model,[16] however, in a form which is mathematically more convenient for our purpose.

The density of the scattering particles is described as

$$n(r) = n_\infty(r) B(r) \qquad \text{with } B(r) = \Theta(\vec{n}r), \qquad (1)$$

where Θ is the Heaviside unit step function. The product form of this density leads to a folding of the infinite-crystal scattering amplitude with a CTR function:

$$F(G) = F_\infty(G) * B_G. \qquad (2)$$

Here G are reciprocal lattice vectors and $F_\infty(G)$ is the structure factor of the infinite crystal. Using the Fourier transform of the Heaviside step function,[17] one finds for the CTR function,

$$B_G = \delta(Q_1)\delta(Q_2)\sqrt{\frac{\pi}{2}} \left(\frac{1}{i\pi Q_3} + \delta(Q_3) \right), \qquad (3)$$

with

$$Q_1 = \hat{X}G; \qquad Q_2 = \hat{Y}G; \qquad Q_3 = \vec{n}G. \qquad (4)$$

Here, $\hat{X}$, $\hat{Y}$, $\vec{n}$ represent the unit vectors of the sample coordinate frame, which must be distinguished from the fcc-lattice coordinate frame. It is identical with the laboratory coordinate frame at normal incidence. Equation (4) defines lateral (Q_1, Q_2) and normal (Q_3) directions for reciprocal space vectors.

The scattering amplitude of the infinite crystal is normally described by well-separated peaks in the reciprocal space. Here, we generalize the ideal delta-peak form[14] $F_\infty(G) = \sum_\mathbf{H} F_\mathbf{H} \delta(G - k^\mathbf{H})$ to $F_\infty(G) = \sum_\mathbf{H} F_\mathbf{H} g(G - k^\mathbf{H})$ with the Gaussian peak shape $g(G)$ in the reciprocal space. Generally, $g(G)$ can be peak dependent, but in this work we assume a universal peak shape for the sake of simplicity. This generalized shape can have many microscopic explanations, e.g., crystal disturbances, and contains all peak-broadening

mechanisms in addition to the surface modeled by the body function $B(r)$. The function $g(G)$ with a standard width σ also generates rocking curves with finite width. Integration of the peak intensities in the scattering plane leads to the infinite-crystal rocking curves having the following shape:

$$\rho(Q_3) = \iint dQ_1 dQ_2 \, g^2(G). \qquad (5)$$

This function has a maximum height of $\rho_{max} = 2^{-1}(\sigma\sqrt{2\pi})^{-4}$ and a full width at half maximum (FWHM) of $\Delta Q_3 = 2\sqrt{\ln 2}\,\sigma$ in the momentum space.

Using Eqs. (2)–(5), for the peak intensities in a small-angle diffraction experiment at normal incidence ($k_0 || \vec{n}$, $G_\mathbf{M} \perp \vec{n}$) one obtains

$$I_\mathbf{M} = \iint_{\text{peak M}} dQ_1 dQ_2 \int dQ_3 \, \delta(Q_3) |F(G)|^2$$
$$= \frac{1}{4} \sum_\mathbf{H} \delta_{\mathbf{H},\mathbf{M}} |F_\mathbf{H}|^2 \rho(Q_3^\mathbf{H}) + \frac{1}{2} \sum_{\mathbf{H} \in \Re_\mathbf{M}} \frac{1}{\sigma^2 2\pi} \frac{|F_\mathbf{H}|^2}{(2\pi Q_3^\mathbf{H})^2}$$
$$+ \text{ peak mixing terms.} \qquad (6)$$

Here we have used the following conventions: (1) The measured reflections $\mathbf{M}$ have to be labeled by the coordinates in reciprocal space if they are mainly generated by a volume-allowed peak, otherwise their names are free but should differ from any $\mathbf{H}$. (2) $\mathbf{H}$ is used to label lattice points in the reciprocal space. (3) $\Re_\mathbf{M}$ is the class of reciprocal lattice points with the same lateral momentum, i.e., $\Re_\mathbf{M} = \{\mathbf{H} | Q_1^\mathbf{H} = Q_1^\mathbf{M}, Q_2^\mathbf{H} = Q_2^\mathbf{M}, Q_3^\mathbf{H} \neq Q_3^\mathbf{M}\}$.

Equation (6) means that the peaks can be visible either because they fulfill Bragg's law (volume signal) or because they belong to a CTR (surface signal). It is interesting that this form of the CTR theory delivers the ratio of surface and volume signals directly. Let $\mathbf{M}v$ be a volume-allowed reflection and $\mathbf{M}s$ a surface reflection generated by the different contributions $I_{\mathbf{M}sn} = |F_{\mathbf{M}sn}|^2 / (\sqrt{2\pi}^3 \sigma Q_3^{\mathbf{M}sn})^2$. Then, the ratio of their intensities is

$$\frac{I_{\mathbf{M}sn}}{I_{\mathbf{M}v}} = \left| \frac{F_{\mathbf{M}sn}}{F_{\mathbf{M}v}} \right|^2 \left| \frac{G^{\mathbf{M}v}}{Q_3^{\mathbf{M}sn}} \right|^2 \frac{(\Delta\omega^{\mathbf{M}v})^2}{2\pi \ln 2}. \qquad (7)$$

To get this expression we used $\rho(Q_3^{\mathbf{M}v}) = \rho(0) = \rho_{max}$ and $\Delta Q_3 = |G^{\mathbf{M}v}| \cdot \Delta\omega^{\mathbf{M}v}$. Thus, the angular width (FWHM) $\Delta\omega^{\mathbf{M}v}$ of the volume-allowed reflections in the rocking curves turns out to be a decisive parameter for the amplitude ratio in Eq. (7). For the $2\bar{2}0$-type peaks we have measured $6°$ (0.12 rad) which is high in comparison to atomic crystals. Therefore, the peak ratio is not necessarily a small number. The other parameters entering the measured amplitude ratio are a ratio of peak amplitudes in reciprocal space and a ratio of k vectors. Both are mostly in the order of unity, but they can also be larger. So, the disadvantage of being a surface reflection [factor $(\Delta\omega^{\mathbf{M}v})^2 / 4.36$] could be compensated.

In the present case we see reflections connected with nonlattice $\frac{1}{3}\{2\bar{4}2\}$ positions in addition to the dominating $2\bar{2}0$-type reflections. At these positions, for example, the reciprocal lattice points $\{11\bar{1}\}$, $\{200\}$, and $\{220\}$ could generate surface signals. Let us calculate the ratio of the different signals for $\mathbf{M}v = 2\bar{2}0$ and $\mathbf{M}sn = 11\bar{1}$ as an example. One finds $|G^{\mathbf{M}v}| = 2\sqrt{2} \times 2\pi/a$, $Q_3^{\mathbf{M}sn} = 1/\sqrt{3} \times 2\pi/a$, $|F_{2\bar{2}0}| = 0.076|F_{000}|$,
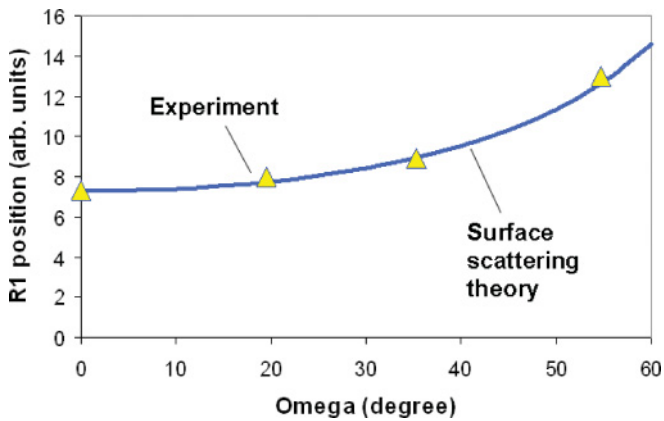
FIG. 2. (Color online) Small-angle x-ray diffraction data from Ref. 9. The position of the $R1$ peak is shifting. The solid line would result from surface scattering of the $\Re_{\mathbf{M}}$ class containing $(11\bar{1})$.

and $|F_{11\bar{1}}| = 0.12|F_{000}|$ for the ideal opal using a textbook formula for the involved atomic form factors.[18] Then one finds $I_{\mathbf{M}sn}/I_{\mathbf{M}v} \approx (1.58 \times 2\sqrt{6} \times 0.12)^2/4.36 = 0.20$, which is surprisingly high.

For atomic-scale crystals, the surface signals are much weaker than the volume signals. However, as we saw, colloidal crystals have relatively broad peaks in reciprocal space likely because of disorder effects. This strongly diminishes especially the volume signals but the surface signals, not as much. The difference occurs because the pure Ewald sphere construction cuts out only a small part of the peak in reciprocal space, whereas the CTR integrates first over the whole peak before a part of the surface rod becomes visible. This may explain why the intensity of the surface peaks can be comparable with the volume peaks.

Of course, the above consideration does not prove that any peak is generated by the surface, but it shows that surface effects have to be considered in the peak assignment. Let us have a closer look at one of the already mentioned publications[9] on diffraction experiments with photonic crystals. Here, peaks at volume-forbidden low-angle fcc positions are clearly visible and have been labeled as $R1$. They have been assigned to additional lattices hypothetically contaminating the photonic crystal. This is a possible explanation, but not the only one. Figure 2 shows the position of these peaks in comparison with the position predicted by surface scattering, which is a $\cos^{-1}$ behavior.

As we can see, the $R1$ peaks found in this work do shift as predicted by the surface scattering theory. Again, this coincidence is no proof but a good hint that these peaks are at least partially generated by the surface. The importance of surface scattering and, in particular, of CTRs has also been

recognized when studying thin inorganic films,[19] molecular crystals,[20] and individual quantum wires.[21] In these examples small scattering volumes generate the diffraction pattern. Such a situation is also realized in artificial opal films. Also, for nanoclusters[22] and quantum dots on surfaces one can expect related effects.

Another aspect should also be mentioned in this Brief Report. In the peak assignment, the 002-type peaks have sometimes[9] been excluded because of a very low atomic form factor. This almost extinction of the peak is by chance. The form factor for a homogeneous sphere crosses zero for QR values of 1.4303π (a solution of $\tan x = x$), whereas the 002 peak has a QR of $\sqrt{2}\pi$. However, this almost coincidence is only true for an ideal opal. Real opal systems show sintering effects between the spheres, fluctuating sphere sizes, and radial dependent porosities of the spheres. These effects change the lattice constants and destroy the homogeneous-sphere model.

The first effect (sintering) can be estimated by a simplified model in which an s part of the sphere radius is involved in the sintering. The overlapping regions of the initial spheres are simply assumed to be compressed. The width of this region is then $2sR$. Using a power expansion around the extinction point ($QR = 1.4303\pi$), one finds for the peak intensity $I_{002} \approx I_{000}(0.644s - 0.00732)^2$. Experimental findings demonstrated realistic sintering values of $s \approx 0.05$.[23] This means that the peaks have much more intensity after sintering than in the nonsintered ideal case ($s = 0$).

Furthermore, the approximation of the real system by simplified sintering of homogeneous spheres is likely not sufficient. The spheres may contain differently structured surfaces (porous or denser) and their sintering behavior is very complex. Also, the inversion process used in many works can induce further modifications.[24] Here, models with core-shell spheres can be regarded as a next step of approximation. Then the 002 reflection also gains much intensity and can become comparable with the other reflections.

In summary, the occurrence of volume-forbidden reflections does not necessarily point to polycrystalline samples. Moreover, for the opal samples which are normally slightly distorted, the occurrence of surfaces peaks is very likely. These peaks can have an intensity which is only five times lower than the strongest volume peaks.

*Corresponding author: marlow@mpi-muelheim.mpg.de

[1]R. M. Amos, J. G. Rarity, P. R. Tapster, T. J. Shepherd, and S. C. Kitson, Phys. Rev. E **61**, 2929 (2000).

[2]P. Jiang, J. F. Bertone, K. S. Hwang, and V. L. Colvin, Chem. Mater. **11**, 2132 (1999).

[3]M. A. McLachlan, N. P. Johnson, R. M. De La Rue, and D. W. McComb, J. Mater. Chem. **14**, 144 (2004).

[4]H.-L. Li, W. Dong, H.-J. Bongard, and F. Marlow, J. Phys. Chem. B **109**, 9939 (2005).

[5]A. V. Petukhov, D. G. A. L. Aarts, I. P. Dolbnya, E. H. A. de Hoog, K. Kassapidou, G. J. Vroege, W. Bras, and H. N. W. Lekkerkerker, Phys. Rev. Lett. **88**, 208301 (2002).

[6] A. V. Petukhov, I. P. Dolbnya, D. G. A. L. Aarts, G. J. Vroege, and H. N. Lekkerkerker, Phys. Rev. Lett. **90**, 028304 (2003).

[7] S. M. Clarke, A. R. Rennie, and R. H. Ottewill, Langmuir **13**, 1964 (1997).

[8] J. H. J. Thijssen, A. V. Petukhov, D. C. 't Hart, A. Imhof, C. H. M. van der Werf, R. E. I. Schropp, and A. van Blaaderen, Adv. Mater. **18**, 1662 (2006).

[9] A. Sinitskii, V. Abramova, N. Grigorieva, S. Grigoriev, A. Snigirev, D. V. Byelov, and A. V. Petukhov, EPL **89**, 14002 (2010).

[10] S. V. Grigoriev, K. S. Napolskii, N. A. Grigoryeva, A. V. Vasilieva, A. A. Mistonov, D. Yu. Chernyshov, A. V. Petukhov, D. V. Belov, A. A. Eliseev, A. V. Lukashin, Yu. D. Tretyakov, A. S. Sinitskii, and H. Eckerlebe, Phys. Rev. B **79**, 045123 (2009).

[11] M. Muldarisnur and F. Marlow, J. Phys. Chem. C **115**, 414 (2011).

[12] H.-L. Li and F. Marlow, Chem. Mater. **17**, 3809 (2005).

[13] S. Förster, A. Timmann, C. Schellbach, A. Frömsdorf, A. Kornowski, H. Weller, S. V. Roth, and P. Lindner, Nat. Mater. **6**, 888 (2007).

[14] C. Giacovazzo, in *Fundamentals of Crystallography*, edited by C. Giacovazzo (Oxford University Press, New York, 1998), p. 141.

[15] A. Authier, Lect. Notes Phys. **112**, 236 (1980).

[16] I. K. Robinson, Phys. Rev. B **33**, 3830 (1986).

[17] R. Bracewell, *The Fourier Transform and Its Applications* (McGraw-Hill, New York, 1965).

[18] R. J. Roe, *Methods of X-Ray and Neutron Scattering in Polymer Science* (Oxford University Press, New York, 2000).

[19] O. Hellwig and H. Zabel, Physica B **283**, 228 (2000).

[20] Y. Wakabayashi, J. Takeya, and T. Kimura, Phys. Rev. Lett. **104**, 066103 (2010).

[21] J. Stangl, C. Mocuta, A. Diaz, T. H. Metzger, and G. Bauer, ChemPhysChem **10**, 2923 (2009).

[22] O. M. Yefanov, A. V. Zozulya, I. A. Vartanyants, J. Stangl, C. Mocuta, T. H. Metzger, G. Bauer, T. Boeck, and M. Schmidbauer, Appl. Phys. Lett. **94**, 123104 (2009).

[23] I. Popa and F. Marlow, ChemPhysChem **9**, 1541 (2008).

[24] F. Marlow and W. Dong, ChemPhysChem. **4**, 549 (2003).